



Biodegradable Mg corrosion and osteoblast cell culture studies

YeoHeung Yun ^{a,*}, Zhongyun Dong ^a, Dianer Yang ^a, Mark J. Schulz ^a, Vesselin N. Shanov ^a, Sergey Yarmolenko ^b, Zhigang Xu ^b, Prashant Kumta ^c, Charles Sfeir ^c

^a University of Cincinnati, Cincinnati, OH, 45221 USA

^b North Carolina A&T SU, Greensboro, NC, 27358 USA

^c University of Pittsburgh, Pittsburgh, PA, 15261 USA

ARTICLE INFO

Article history:

Received 3 December 2008

Received in revised form 14 January 2009

Accepted 11 February 2009

Available online 25 February 2009

Keywords:

Biodegradable implant

Corrosion

U2OS cells

ABSTRACT

Magnesium (Mg) is a biodegradable metal that has significant potential advantages as an implant material. In this paper, corrosion and cell culture experiments were performed to evaluate the biocompatibility of Mg. The corrosion current and potential of a Mg disk were measured in different physiological solutions including deionized (DI) water, phosphate-buffered saline (PBS), and McCoy's 5A culture medium. The corrosion currents in the PBS and in the McCoy's 5A-5% FBS media were found to be higher than in DI water, which is expected because corrosion of Mg occurs faster in a chloride solution. Weight loss, open-circuit potential, and electrochemical impedance spectroscopy measurements were also performed. The Mg specimens were also characterized using an environmental scanning electron microscope and energy-dispersive X-ray analysis (EDAX). The X-ray analysis showed that in the cell culture media a passive interfacial layer containing oxygen, chloride, phosphate, and potassium formed on the samples. U2OS cells were then co-cultured with a Mg specimen for up to one week. Cytotoxicity results of magnesium using MTT assay and visual observation through cell staining were not significantly altered by the presence of the corroding Mg sample. Further, bone tissue formation study using von Kossa and alkaline phosphatase staining indicates that Mg may be suitable as a biodegradable implant material.

© 2009 Elsevier B.V. All rights reserved.

1. Introduction

Implants such as bone fixation plates, stents, screws, and wires are typically fabricated using corrosion resistant metals such as stainless steels, Ti, and Co-Cr-based alloys [1–3]. These implants remain in the body permanently although often they are no longer needed. Biodegradable polymers and resorbable ceramics have been explored as alternatives to permanent implants. However, biodegradable polymers and ceramics may not provide sufficient strength, ductility, and bioabsorbability for orthopedic applications. Iron (Fe) and magnesium (Mg) are two metals that are biodegradable. Ideally, a biodegradable metal should degrade in the biological system at a desired rate and not be toxic or adversely affect the already existing metal-organic molecules and enzymes existing in the physiological environment [4–20]. Also, the metal should not harmfully interact with the external environment and should not be antigenic (cause an adverse immune response). The mechanical properties of Mg are close to the properties of bone. For example, the Young's modulus and density of magnesium are 45 GPa and $0.74 \text{ g} \cdot \text{cm}^{-3}$, respectively, these properties compare satisfactorily to the elastic modulus and density of human bone which are 10–15 GPa and $1.5\text{--}2.0 \text{ g} \cdot \text{cm}^{-3}$, respectively.

The elastic modulus and density of Fe, 91 GPa and $7.8 \text{ g} \cdot \text{cm}^{-3}$ respectively, are not as similar to bone. However, Fe is being considered for implants in certain applications (e.g. biocorrosible iron stents [20]). Of late, Mg and its alloys are the most studied metal for use as biodegradable implants because of their potential non-toxicity, similar mechanical properties to bone, biocompatibility, and biodegradability [4–11,24–26]. The similar mechanical properties will minimize stress shielding effects that occur when Mg-based implants are used to reinforce bone. Actually, the mechanical properties of biodegradable implants change with time as the Mg dissolves in the physiological fluids while bone cells migrate and replace the Mg with

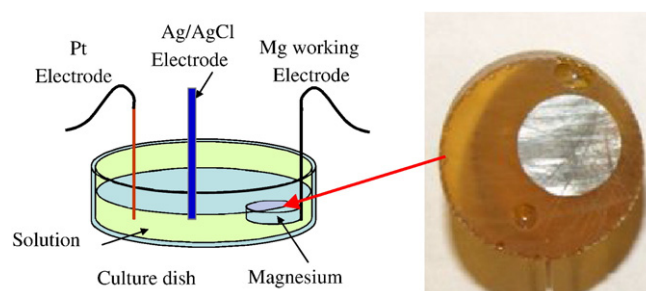


Fig. 1. Electrochemical sensor used for corrosion analysis and bone cell co-culturing.

* Corresponding author.

E-mail address: yunyg@email.uc.edu (Y. Yun).

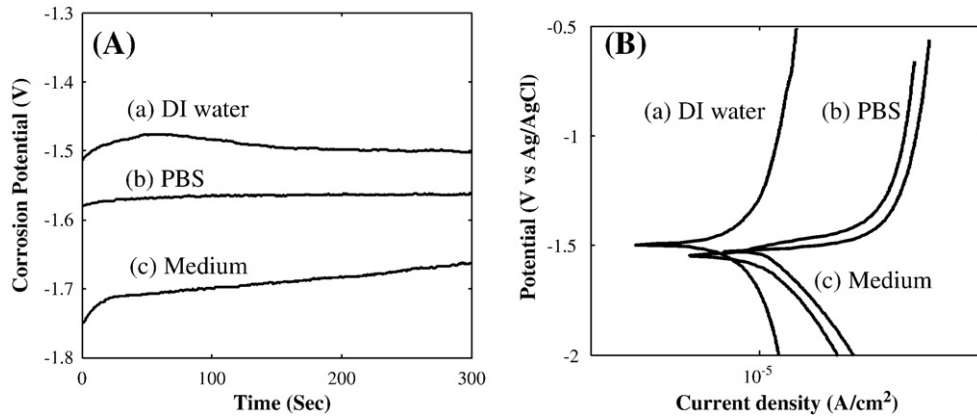


Fig. 2. Corrosion behavior of Mg: (A) Open circuit potential and (B) potentiodynamic polarization curves of Mg measured in different solutions: (a) DI water, (b) PBS, and (c) McCoy's 5A medium containing 5% FBS. The scan rate was 5 mV/s.

host tissue. The corrosion of Mg and simultaneous bone deposition is a complex process, and this interaction is considered an area where new sensors and modeling are needed. The by-products of corrosion (chemicals, gas, and possibly particles) are released into the body as the implant corrodes. Assessment of the effect of these corrosion products on bone cells is very much needed. In addition, time dependant electrochemical characterization of Mg in different solutions coupled with *in vitro* testing [8,10–16] is needed to understand the applicability of the Mg implant material.

Mg may be the most suitable base material for biodegradable implants because Mg is biocompatible, biodegradable, lightweight, strong, and ductile. The most important property that a Mg-based implant provides is initial mechanical strength and to act as a scaffold that safely dissolves into the blood stream while bone cells migrate and replace the metal with host tissue. Biodegradable metals such as Mg and its alloys could provide many advantages for craniofacial and orthopedic implants, cardiovascular devices, musculo-skeletal surgery, and other applications [4–8]. Mg can decrease implant size, reduce stress concentrations at the interface between the implant and bone, reduce healing time for bone fracture, and eliminate surgery for implant removal. Bioabsorbable Mg stents would leave behind only the healed natural vessel and free patients from carrying metal prostheses in their coronary arteries [24]. Mg vascular implants degradable by biocorrosion could replace permanent implants. Biodegradable implants may stimulate bone regeneration to repair birth defects such as cleft lip (an upper lip congenitally divided into two parts) and cleft palate (a congenital fissure along the midline of the roof of the mouth), and craniosynostosis (irregular joints between the cranial bony plates fuse together), and will be important for surgical applications such as spine fusion and nonunion of fractures [25,26]. Beneficial metals should also be alloyed in Mg to strengthen resorbing bone at the implant.

In terms of benefit to society, engineering of metallic biomaterials is a new field of research that is predicted to have widespread applications. Alloys and porous implants may also deliver minerals and drugs to promote bone healing and increase the creep resistance, tensile strength, and corrosion resistance of implants. Overall, a large number of combinations of binary and ternary Mg alloys can be developed for implants to do what we want them to do inside the

body. Developing biodegradable metals also supports development of auxiliary technologies to repair or enhance the performance of the body such as implantable bionic devices and biosensors.

To allow all these technologies go forward, quantitative knowledge of the electrochemical properties and corrosion behavior of Mg in physiological solutions is needed. In particular, electrochemical analysis of the passivation layer forming on the Mg surface in different solutions will help to understand the self-regulating behavior of corrosion. The effect of Mg corrosion on bone cell viability and biocompatibility must also be studied including cellular alkaline phosphatase production and mineralization. Initial studies in these areas are reported in this paper.

2. Corrosion analysis

Mg (99.95%, Kurt J. Lesker) pellets 6 mm diameter and 8 mm long were polished at the ends and cast into epoxy (Resin 862 and EPICURE curing agent W). The bottom surface of the specimen was polished and conducting epoxy was used to connect a Cu wire to the Mg. Then, the conductive epoxy was covered with insulating epoxy. The top

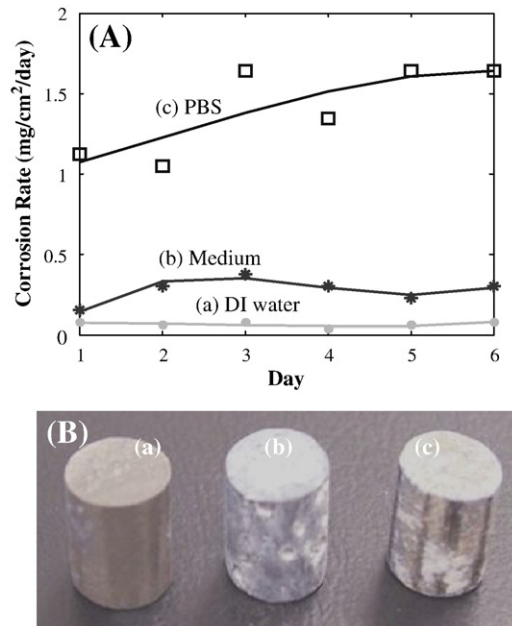


Fig. 3. (A) Mg weight loss in different solutions: (a) DI water; (b) McCoy's 5A-5% FBS; and (c) PBS. (B) Specimens after exposure to different solutions for 5 days: (a) DI water; (b) PBS, and (c) McCoy's 5A-5% FBS.

Table 1
Electrochemical analysis data for magnesium in different solutions.

	OCP (V)	R _{et} (KΩ)	I _{corr} (μA/cm ²)	E _{corr} (V)
DI water	-1.48	3.591	0.006	-1.40
PBS	-1.57	0.793	2.35	-1.53
McCoy's 5A Medium	-1.69	1.037	0.58	-1.55

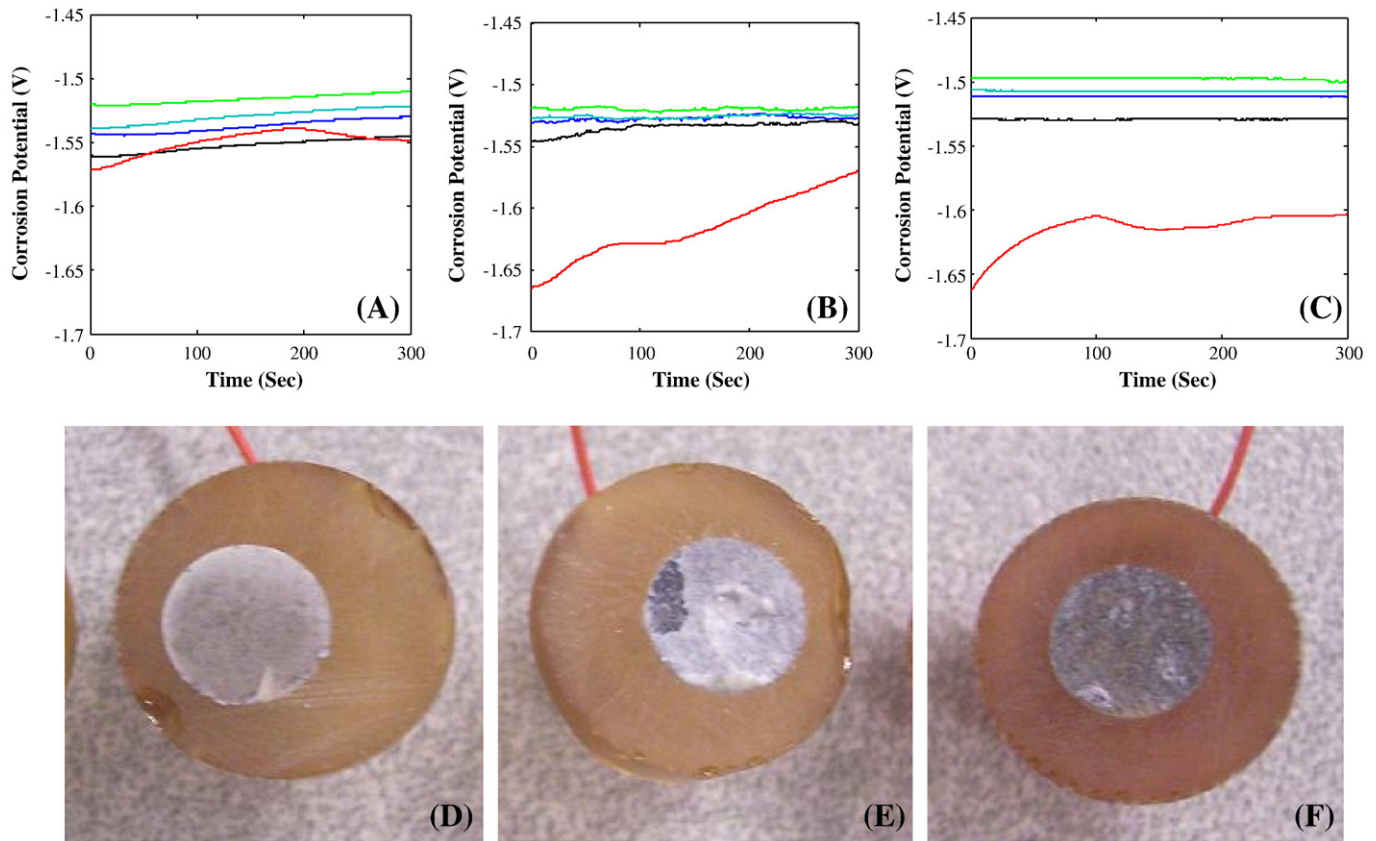


Fig. 4. Time-dependent measurement of the open circuit potential and the pictures of specimens after exposure to different solutions for 5 days at 37 °C in different solutions: (A, D) in DI water, (B, E) in PBS, and (C, F) in McCoy's 5A-5% FBS. The measurements were made for 300 s on different days (red is day 1, black is day 2, blue is day 3, cyan is day 4, and green is day 5). (For interpretation of the references to color in this figure legend, the reader is referred to the web version of this article.)

surface of the specimens was polished using a diamond slurry (Microid Diamond Compound, Lot #34201, Leco) to expose a fresh area of Mg. Then the magnesium samples were ultrasonically cleaned in ethanol and blown dry with a stream of nitrogen. McCoy's 5A medium with L-glutamine was purchased from Lonza Group Ltd (Cat No 12-88F, Switzerland) and fetal bovine serum (FBS) was purchased from MA Bioproducts (Walkersville, MD).

In order to evaluate the electrochemical corrosion properties of magnesium, electrochemical measurements including open circuit potential, potentiodynamics, polarization resistance, and electrochemical impedance spectroscopy (EIS) were made using a Gamry Potentiostat (model: PCI4/750) coupled with the DC105 and EIS-300 software [23]. Three electrodes: an Ag/AgCl reference electrode,

a Mg working electrode, and a platinum counter electrode were used, as shown in Fig. 1.

2.1. Corrosion electrochemistry

Fig. 2 shows the open-circuit potential (OCP) and potentiodynamic polarization curves of the epoxy Mg pellet measured in different solutions: (a) DI, (b) PBS, and (c) McCoy's 5A medium containing 5% FBS at 37 °C. Based on the measurements in Fig. 2, the electrochemical parameters representing the Mg corrosion behavior in different solutions were curve fit to the experimental data to provide a model of the corrosion behavior for design purposes and are listed in Table 1. Here OCP is the open circuit potential, R_p is the

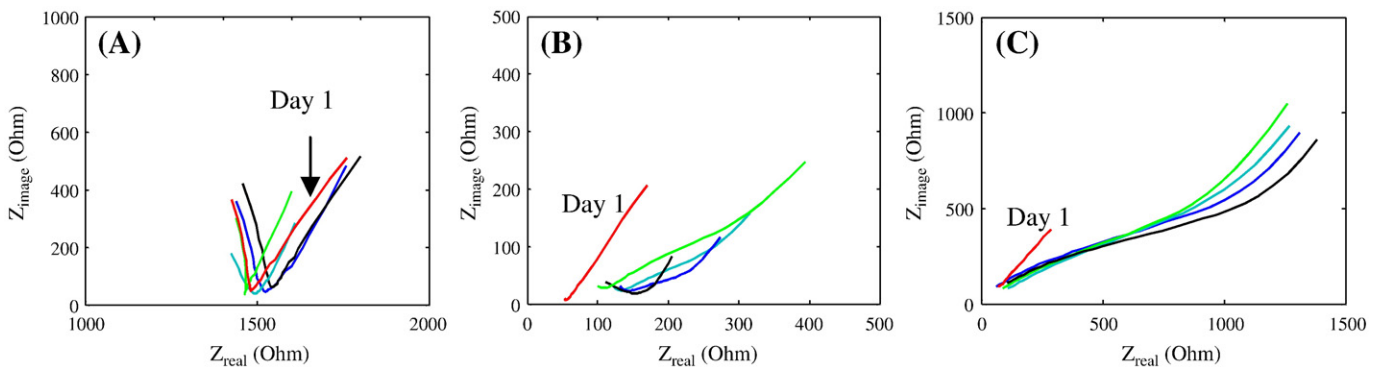


Fig. 5. Time-dependent EIS measurement in different solutions: (A) DI; (B) PBS; and (C) McCoy's 5A-5% FBS. The magnesium specimens were incubated for 5 days at 37 °C. EIS was done with a sinusoidal potential magnitude of ± 5 mV at frequencies between 100 Hz and 100 kHz (red is day 1, black is day 2, blue is day 3, cyan is day 4, and green is day 5). (For interpretation of the references to color in this figure legend, the reader is referred to the web version of this article.)

Table 2

Estimated EIS parameters for magnesium in different solutions.

		Day 1	Day 2	Day 3	Day 4	Day 5
PBS	R_c (Ω)	0	64	119	182	264
	C_c (μF)	0	1.65	1.52	1.47	1.38
McCoy's 5A Medium	R_c (Ω)	0	789	791	810	822
	C_c (μF)	0	41	44	39	40

polarization resistance, I_{corr} is the corrosion current density, and E_{corr} is the corrosion potential of magnesium.

The standard corrosion potential of magnesium (Mg^{2+}/Mg) at 25 °C is -2.37 V. However, the actual corrosion potential was -1.53 V in PBS solution. G. Song et al. [9] suggested that magnesium forms a magnesium hydroxide film which inhibits direct contact of the magnesium with the solution. This film may also cause the measured corrosion potential to be larger (more noble) than the theoretical value. The corrosion potential, E_{corr} of magnesium in DI water -1.4 V is higher (more noble) than the corrosion potential of magnesium in PBS solution -1.53 V and in McCoy's 5A medium -1.55 V. This means the corrosion of magnesium occurs more slowly in DI water. The corrosion potentials for magnesium in PBS and McCoy's 5A medium were measured to be about the same. However, the corrosion current density I_{corr} of magnesium in PBS was four times greater than the corrosion current density of magnesium in McCoy's 5A-5% FBS (results in Table 1). The polarization resistance also called the electron transfer resistance, R_{et} , evaluates the ability of the material to resist corrosion and it is inversely related to the corrosion current. The same phenomenon of greater corrosion occurring in the PBS solution than in the McCoy's 5A-5% FBS is also represented in the polarization resistance measurement. Probably the passivation layer formation on the magnesium in the McCoy's 5A-5% FBS inhibits the corrosion.

Indeed, R. Rettig et al. [12] reported that albumin or other proteins created a blocking layer on the surface in the first hours of exposure.

2.2. Corrosion weight loss measurement

Mg specimens were immersed in individual 30 mL solutions of DI water, PBS, and McCoy's 5A-5%FBS at 37 °C. The specimens were removed from the solution and dried in air, but not lyophilized, and the weight loss was measured each day. To simulate the *in vivo* condition, the surface corrosion was not removed from the specimens. Fig. 3(A) shows Mg weight loss with time. In the future, a plot of corrosion vs. time will be prepared to show the bulk degradation. The Mg weight loss in PBS solution is greater than with McCoy's 5A-5% FBS or DI water. Even the pitting behavior of Mg can be seen in the PBS solution (Fig. 3B(c)).

Mg weight loss in the medium increased for 3 days and then leveled off at constant rate of 0.3 mg/cm²/day. Balancing the corrosion action and passive layer formation on the surface might be the reason for the steady-state response.

2.3. Open circuit potential

Time-dependant measurement of the open circuit potential in different solutions: DI, PBS, and McCoy's 5A-5% FBS is shown in Fig. 4. After immersing the magnesium specimens in different solutions for 1 day, the open circuit potential of magnesium in PBS and in the medium dramatically decreased and then approached a constant value probably due to formation of the passivation layer. Note that overall the corrosion potential becomes more positive (closer to zero) with time. Fig. 4(D–F) shows the magnesium specimens after immersion for 5 days. The passivation layer on the surface is visible.

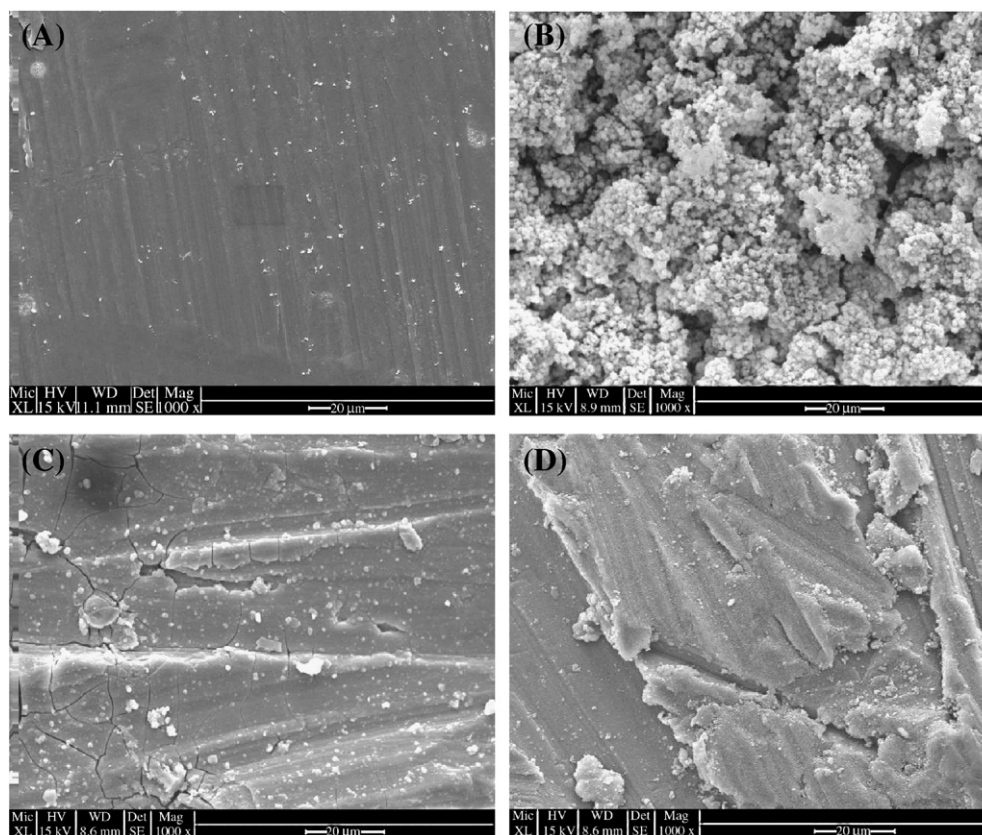


Fig. 6. ESEM images of: (A) the Mg surface and (B–D) the corroded Mg surface after exposure for 5 days in different solutions; (B) DI water, (C) PBS, and (D) McCoy's 5A medium containing 5% FBS.

2.4. Time dependent electrochemical impedance

Fig. 5 shows the complex electrochemical impedance behavior of magnesium in different solutions for 5 days. The solution resistance is the value Z_{real} which occurs when the imaginary part of impedance Z_{imag} is equal to zero. The solution resistance for magnesium in the three solutions was calculated based on measurements made on the first day. As shown in Fig. 5(A), the solution resistance of magnesium in DI water is about 1.5 K Ω . There is not much change in impedance with time. In the case of Fig. 5(B) and (C), a compressed semicircle started to form from the second day on and the diameter of the semicircle kept increasing with time. This semicircle corresponds to a passive layer forming on the magnesium surface and can be modeled with a parallel coating capacitance, C_c , and resistance, R_c . Impedance parameters obtained from non-linear curve-fitting of the experimental results to (1) are shown in Table 2. The coating resistance and capacitance of the magnesium in the McCoy's 5A-5% FBS is quite large and stable with time. These results explain the creation of a uniform passive interfacial layer on the magnesium surface. The higher values of resistance and capacitance in the medium as compared to the PBS solution are probably caused by formation of a uniform interfacial

layer containing chemicals from McCoy's 5A-5% FBS. In the future, this same electrochemical impedance spectroscopy (EIS) analysis will be repeated to characterize and model the cells plating on the implant.

2.5. Microscopy and chemical analysis of corrosion

Based on the hypothesis that a passivation layer formed on the surface, environmental scanning electron microscopy (ESEM) with energy dispersive X-ray (EDX) analysis was done to analyze the surface after 5 days incubation. Fig. 6 shows ESEM images of: (A) the Mg surface and (B–D) the corroded Mg surface after 5 days in different solutions: (B) DI water, (C) PBS, and (D) McCoy's 5A-5% FBS. A porous surface of Mg is interestingly formed when it was incubated in DI water. However, a passive interfacial layer was not found. As shown in Fig. 6(C–D), a thin (2–5 μm) passive layer is formed which might be the reason for slowing corrosion of the surface of the Mg. EDX analysis was performed and only a Mg peak was observed for the DI case. However, oxygen, chloride, phosphate, and potassium peaks were observed for the other solutions. Probably the interaction between Mg and the solution created a passive interfacial layer using chemicals in the solution.

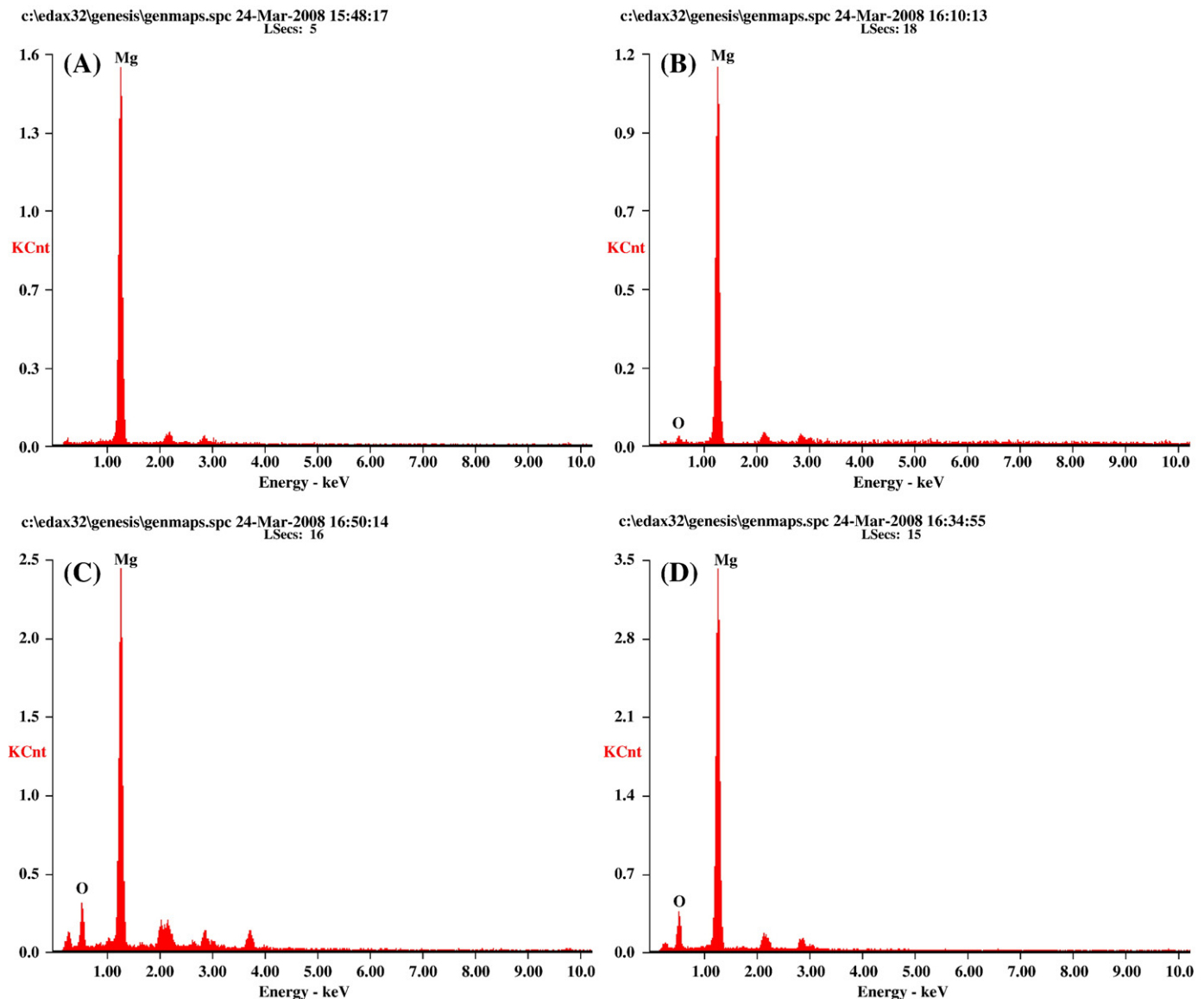


Fig. 7. EDX analysis of: (A) the clean magnesium surface; and (B–D) the corroded magnesium surface after 5 days exposure in different solutions; (B) DI water, (C) PBS, and (D) McCoy's 5A-5% FBS.

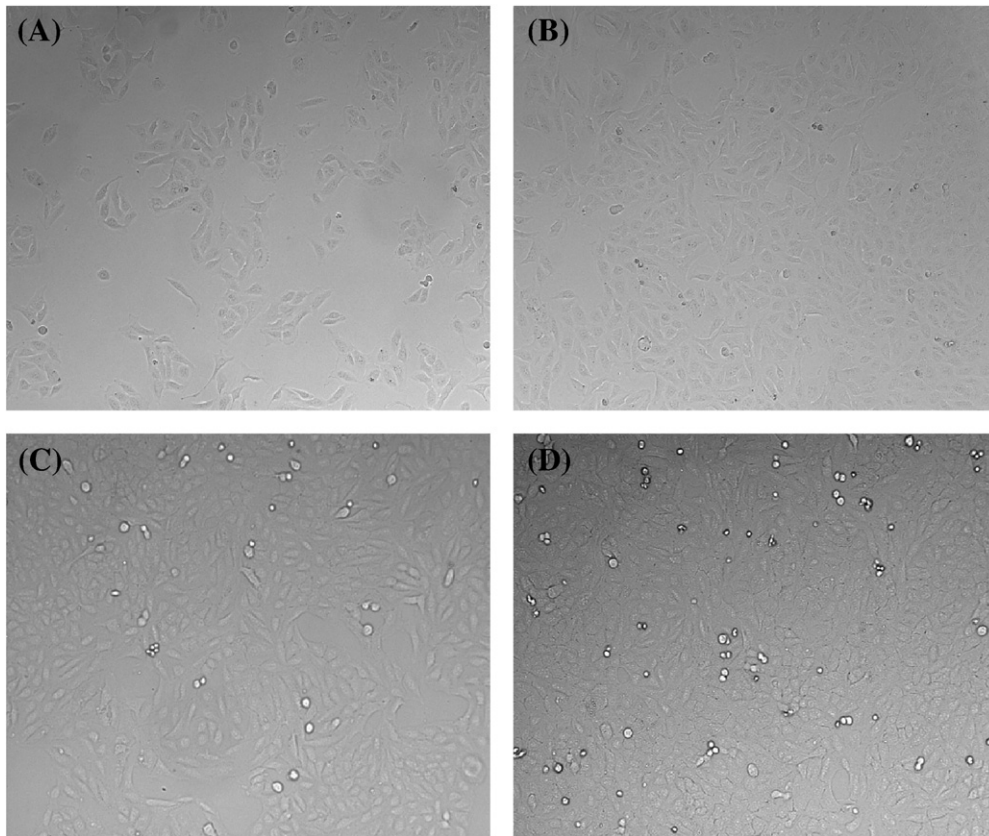


Fig. 8. Bright field images of U2OS cells cultured as: (A, C) controls and co-cultured with (B, D) magnesium specimens. Images were taken at (A, B) the first day and (C, D) the fifth day.

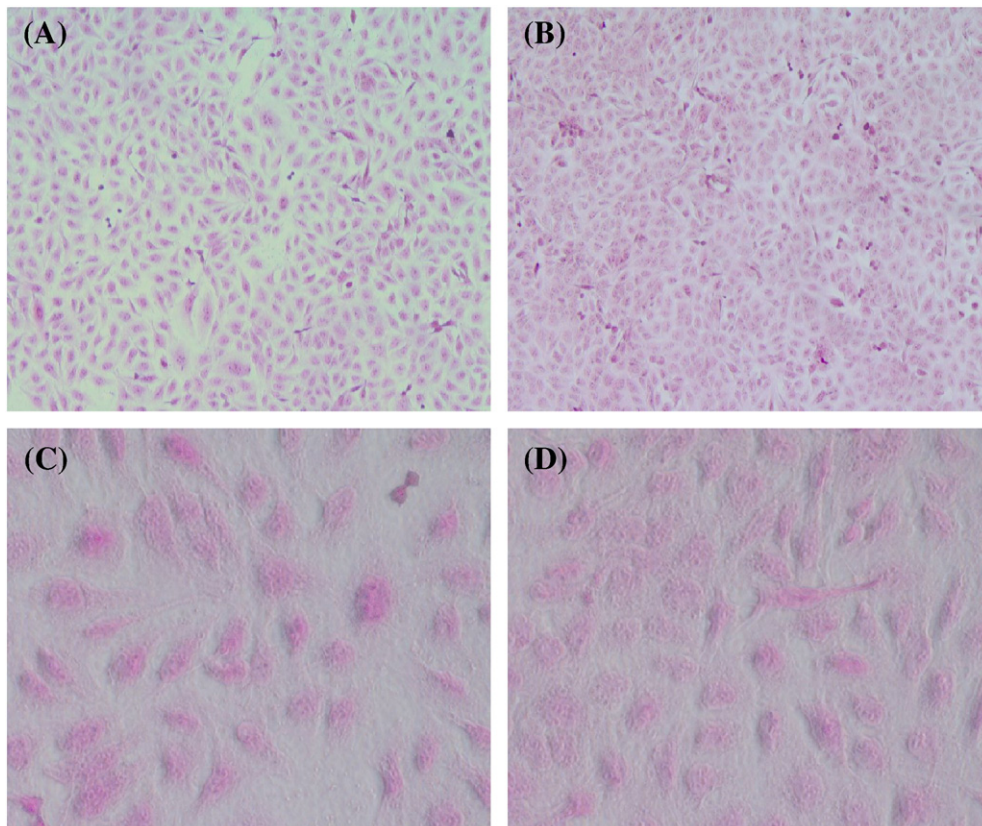


Fig. 9. ALP staining of an adherent U2OS cell after 5 days incubation. U2OS cells were (A, C) cultured as controls and (B, D) co-cultured with magnesium. (Magnification (A, B) 10× and (C, D) 40×). (For interpretation of the references to color in this figure legend, the reader is referred to the web version of this article.)

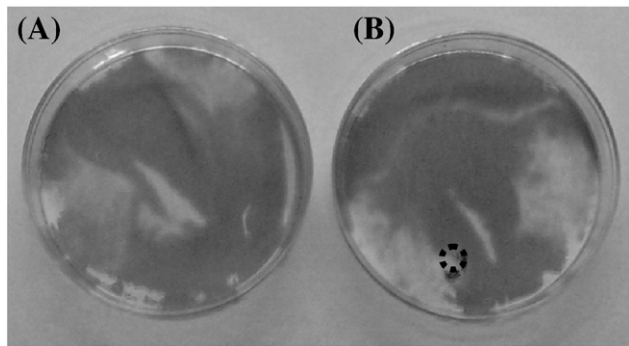


Fig. 10. von Kossa staining of adherent U2OS cells to see mineralization nodules. U2OS cells were: (A) cultured as a control; and (B) co-cultured with a Mg specimen (specimen placed in the dotted area). von Kossa staining was done after 10 days incubation.

Fig. 7 shows EDX analysis of: (A) the magnesium surface and (B–D) the corroded magnesium surface after 5 days exposure in different solutions: (B) DI water, (C) PBS, and (D) McCoy's 5A-5% FBS. Only a magnesium peak was observed in Fig. 7(A). However, oxygen, chloride, phosphate, and potassium peaks were observed in Fig. 7 (C) and (D), which show the composition of the passive layer. Probably the interaction between magnesium and the solution created a passive interfacial layer using chemicals in the solution.

Fig. 8 shows *in vitro* results demonstrating that growth of U2OS cells was not significantly altered by magnesium. It appears that the presence of magnesium affected neither cell proliferation nor cell viability. Moreover, Zijian Li et al. [7] reported that Mg–Ca alloy stimulated the growth of L-929 cells since magnesium ions enhance the adhesion of human bone-derived cells which express enhanced levels of the $\alpha 5\beta 1$ - and $\beta 1$ -integrin receptor. Even though we can see alkalization of the medium, the *in vitro* results showed that magnesium did not affect cell viability. The medium turned a bright pink color and pH was around 8.1.

3. Cell viability and mineralization

U2OS cells (osteoblast cells [17]) were cultured at 37 °C with 5% CO₂ in McCoy's 5A-5% FBS with ascorbic acid. U2OS cells in their exponential growth phase were harvested in 1-min and treated with a 0.25% trypsin and 0.02% EDTA solution. U2OS cells were then seeded in culture dishes (60 mm × 15 mm) with a density of 100,000 cells per dish (28 cm²). After an overnight incubation, the cells were cultured in the presence of a sterilized Mg specimen system (as illustrated in Fig. 1). Only the top surface of the Mg specimen was exposed (6 mm dia.) to the solution, the other sides were insulated

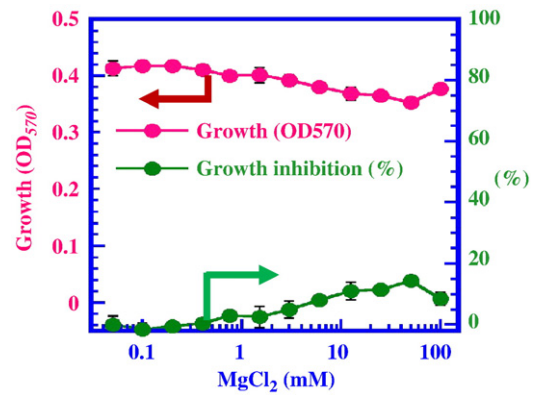


Fig. 12. The effect of Mg chloride concentration on the growth and proliferation of osteoblast. The cells were cultured for 4 days and then evaluated using the MTT assay.

with PDMS (Sylgard 184 PDMS, Dow Corning). The specimen was bonded to the bottom of the culture dish using PDMS.

3.1. Alkaline phosphatase staining

The U2OS cells were washed twice with PBS and fixed in 10% buffered formalin for 1 h. The cultured cells were washed and incubated in 5% silver nitrate solution under light for 1 h. After rinsing with DI water, incubation in 5% sodium thiosulfate was carried out for 2 min and counter-stain with 2.5% fuchsin was completed. The final stained cells were rinsed with DI water and analyzed using a bright field microscope. It is known that alkaline phosphatase (ALP) is an important component in hard tissue formation, and is highly expressed in mineralized tissue cells. U2OS cells were stained and generation of alkaline phosphatase (red) is shown in Fig. 9. There is no discernable difference in alkaline phosphatase activity between the control and the Mg cultured samples. Moreover, it appeared that the presence of Mg did not cause cell lysis or cytotoxicity (Fig. 9).

3.2. von Kossa staining

von Kossa staining is well known in the field of bone research as a method for staining tissue mainly for calcium to indicate bone mineralization. After culturing the U2OS cells for 10 days, the cells were washed twice with PBS and fixed in 10% neutral formalin buffer for 15 min. The cultured cells were washed in distilled water and incubated in distilled water containing Naphthol AS MX-PO4 (sigma, N5000), Tris HCl, and Red Violet LB salt (Sigma F1625) for 45 min. After rinsing with DI water, the cells were incubated in 2.5% silver nitrate for 30 min. Finally the stained cells were rinsed with DI water

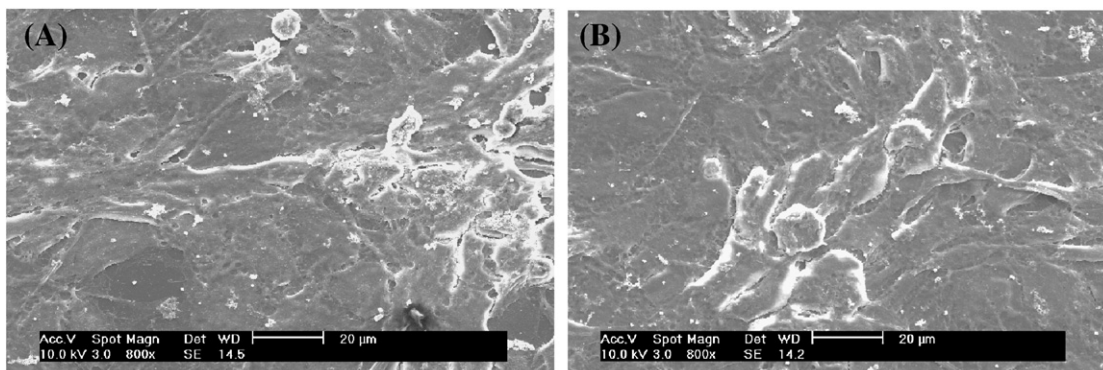


Fig. 11. ESEM images after von Kossa staining of adherent U2OS cells. U2OS cells were: (A) cultured as a control; and (B) co-cultured with a Mg specimen (specimen placed in the dotted area). von Kossa staining was done after 10 days incubation.

and incubated in sodium carbonate formaldehyde for 30 s. In order to verify bone mineralization, von Kossa staining of adherent U2OS cells was done. As shown in Fig. 10, the typical appearance of colonies of cells stained positively with the von Kossa stain is seen in both samples. ESEM was used to explore deeply the mineralization capability of the cells after von Kossa staining. As shown in Fig. 11, we can see the mineralization and cell morphology, however, there was not much difference between two specimens.

3.3. MTT assay

Evaluation of Mg cytotoxicity was performed by the 3-(4,5-dimethylthiazol)-2,5-diphenyltetrazolium bromide (MTT) assay. U2OS cells were seeded at a density of 2×10^3 cells/well in 96-well plates and incubated for 4 days at 37 °C and 5% CO₂. During the final 2 h of incubation, MTT (2 mg/ml PBS, 20 μl/well) was added. The medium was then removed, and dark-blue formazan was dissolved in dimethyl sulfoxide. The absorbance was measured with a 96-well microtiter plate reader (FLUOstar Optima microplate reader) at 570 nm. The percentage of cell growth inhibition was calculated according to the following formula: inhibition (%) = $(1 - A_{570}$ of treated group / A_{570} of control group) $\times 100$, where the OD₅₇₀ of treated group represents the measurement from the wells with different Mg chloride concentration and the OD₅₇₀ of control represents the measurements from the wells treated with PBS buffer only. Effects of Mg on cell growth were further validated in the MTT assay. As shown in Fig. 12, Mg moderately inhibited the growth of U2OS cells only at concentrations above 10 mM.

4. Comparison of permanent and biodegradable implants

The advantages and limitations of different types of implants should be determined in order for patients to make informed decisions on the type of implant best for them. One initial consideration is the difference in size between a permanent implant and a biodegradable polymer implant. The thicker implant may be undesirable for craniofacial and other cosmetic applications. The biodegradable Mg implant would be about the same size as the permanent implant but the biodegradable implant would dissolve after the bone or tissue has healed.

Future research is needed to compare the properties of different implant materials including: (1) non-degradable metal, (2) bioresorbable polymer, (3) biodegradable iron, (4) biodegradable magnesium, and (5) bioresorbable Mg nanocomposites. If materials (3) to (5) are successfully developed, physicians will have an assortment of materials that can meet many applications in regenerative medicine. There is also the possibility to use two biodegradable dissimilar metals (e.g. Fe [22] and Mg) to use galvanic corrosion to control the corrosion properties of an implant [21]. Also, simulation with commercial softwares such as COMSOL might be able to predict environmental change caused by Mg corrosion.

5. Conclusions

Mg was evaluated as a biodegradable implant material. Corrosion of Mg was initially fast and then slowed after 1 day because of the

formation of a passivation layer on the surface. Open circuit potential and polarization resistance measurements also confirmed the passivation layer formation. Preliminary *in vitro* studies revealed that Mg ions released from the Mg specimen did not significantly affect proliferation and viability of U2OS osteoblast cells. Alkaline phosphatase and von Kossa staining showed that expression and enzymatic activity of the phosphatase and mineralization in the osteoblast cells were not significantly altered. Further studies are needed to determine the change in pH, Mg concentration, and hydrogen evolution, which will provide more quantitative results of *in vitro* Mg implant behavior. A media flow system is being developed to allow simulation of the *in vivo* condition. A comparison of different implant materials provides guidance on selecting the best option. Overall, this paper suggests the importance of Mg in future implant applications.

Acknowledgment

This work was sponsored by the NSF ERC *Revolutionizing Metallic Biomaterials*, <http://erc.ncat.edu/>.

References

- [1] C. Li, S. Gao, T. Terashita, T. Shimokawa, H. Kawahara, S. Matsuda, N. Kobayashi, *Cell Tissue Research* 324 (2006) 369.
- [2] P.J. Brugge, S. Dieudonne, J.A. Jansen, *Journal of Biomedical Materials Research* 61 (2002) 399.
- [3] I.V. Branzoi, M. Iordoc, M. Codescu, *Surface and Interface Analysis* 40 (2008) 167.
- [4] M.P. Staiger, A.M. Pietak, *Biomaterials* 27 (2006) 1728.
- [5] J. Vormann, *Molecular Aspects of Medicine* 24 (2003) 27.
- [6] M.N. Helmus, D.F. Gibbons, D. Cebon, *Toxicologic Pathology* 36 (2008) 70.
- [7] Z. Li, X. Gu, S. Lou, Y. Zheng, *Biomaterials* 29 (2008) 1329.
- [8] L. Xu, E. Zhang, D. Yin, S. Zeng, K. Yang, *Journal of Materials Science* 19 (2008) 1017.
- [9] G. Song, A. Atrens, *Advanced Engineering Materials* 5 (2003) 837.
- [10] K.Y. Chiu, M.H. Wong, F.T. Cheng, H.C. Man, *Surface and Coating Technology* 202 (2007) 590.
- [11] W.D. Müller, M.L. Nascimento, M. Zeddies, M. Córscico, L.M. Gassa, M. Mele, *Materials Research* 10 (2007) 5.
- [12] R. Rettig, S. Virtanen, *Journal of Biomedical Materials Research Part A* 85 (2007) 167.
- [13] F. Witte, J. Fischer, J. Nellesen, H. Crostack, V. Kaese, A. Pisch, F. Beckmann, H. Windhagen, *Biomaterials* 27 (2006) 1013.
- [14] Y.H. Yun, Z.Y. Dong, V.N. Shanov, M.J. Schulz, *Nanotechnology* 18 (2007) 465505.
- [15] G. Song, *Corrosion Science* 49 (2007) 1696.
- [16] R. Udhayan, D.P. Bhatt, *Journal of Power Sources* 63 (1996) 103.
- [17] A. Cerovic, I. Miletic, S. Sobajic, D. Blagojevic, M. Radusinovic, A. El-Sohemy, *Biological Trace Element Research* 116 (2007) 61.
- [18] H. Zreiqat, C.R. Howlett, A. Zannettino, P. Evans, G.S. Tanzil, C. Knabe, M. Shakibaei, *Journal of Biomedical Materials Research* 62 (2002) 175.
- [19] S. Grimnes, O. Martinsen, *Bioimpedance and Bioelectricity: Basics*, Academic Press, 2000.
- [20] R. Waksman, R. Pakala, R. Baffour, R. Seabron, D. Helling, F.O. Tio, *Journal of Interventional Cardiology* 21 (2008) 15.
- [21] H. Zitter, K. Pauluzzi, *Journal of Materials Science: Materials in Medicine* 4 (1993) 159.
- [22] J.L. Sandrik, E.H. Greener, *Journal of Biomedical Materials Research* 5 (1971) 283.
- [23] Gamry Instruments, *Electrochemical Corrosion Measurements*. http://www.gamry.com/App_Notes/DC_Corrosion/GettingStartedWithEchemCorrMeasurements.htm.
- [24] P. Erne, M. Schier, T.J. Resink, *Cardiovascular and Interventional Radiology* 29 (2006) 11.
- [25] B. Heublein, R. Rohde, V. Kaese, M. Niemyer, W. Hartung, A. Haverich, *Heart* 89 (2003) 651.
- [26] Z. Lia, X. Gua, S. Loub, Y. Zhenga, *Biomaterials* 29 (2008) 1329.